JACS
JOURNAL OF THE AMERICAN CHEMICAL SOCIETY
Communication
pubs.acs.org/JACS

Slow Magnetic Relaxation in a Mononuclear Eight-Coordinate Cobalt(II) Complex

Lei Chen,[†] Jing Wang,[†] Jin-Mei Wei,[‡] Wolfgang Wernsdorfer,[§] Xue-Tai Chen,*[,†] Yi-Quan Zhang,*[,‡] You Song,*[,†] and Zi-Ling Xue[⊥]

[†]State Key Laboratory of Coordination Chemistry, Nanjing National Laboratory of Microstructures, School of Chemistry and Chemical Engineering, Nanjing University, Nanjing 210093, China

[‡]Jiangsu Key Laboratory for NSLSCS, School of Physical Science and Technology, Nanjing Normal University, Nanjing 210023, China

[§]Nanoscience Department, BP 166, Institut Néel, CNRS, 380412 Grenoble Cedex 9, France

[⊥]Department of Chemistry, University of Tennessee, Knoxville, Tennessee 37996, United States

Supporting Information

ABSTRACT: The quest for the single-molecular magnets (SMMs) based on mononuclear transition-metal complexes is focused on the low-coordinate species. No transition-metal complex with a coordination number of eight has been shown to exhibit SMM properties. Here the magnetic studies have been carried out for a mononuclear, eight-coordinate cobalt(II)-12-crown-4 (12C4) complex $[Co^{II}(12C4)_2](I_3)_2(12C4)$ (**1**) with a large axial zero-field splitting. Magnetic measurements show field-induced, slow magnetic relaxation under an applied field of 500 Oe at low temperature. The magnetic relaxation time τ was fitted by the Arrhenius model to afford an energy barrier of U_{eff} = 17.0 cm^{-1} and a preexponential factor of $\tau_0 = 1.5 \times 10^{-6}$ s. The work here presents the first example of the eight-coordinate, mononuclear, 3d metal complex exhibiting the slow magnetic relaxation.

Single-molecule magnets (SMMs) have been of intense interest over the last two decades due to their novel properties and potential applications in magnetic information storage, quantum computation, and spintronics.[1] Most research efforts are devoted toward the polynuclear magnetic clusters with large ground spin states.[2] In 2003, Ishikawa et al.[3] reported the first mononuclear, lanthanide ion-based SMM with a very high-energy barrier resulting from the strong uniaxial anisotropy of the lanthanide ion, which is subsequently referred to as a single-ion magnet (SIM). So far many mononuclear lanthanide-based and some actinide-based compounds have been reported to exhibit slow magnetic relaxation.[4] More recently the search for new SIMs has been extended to transition-metal ions, including iron(I, II, III),[5−7] cobalt(II),[8] manganese(III),[9] nickel(I),[10] and rhenium(IV)[11] ions.

It is well-known that the magnetic anisotropy can be fine-tuned via the ligand environment. For the transition-metal ions, the ligand-field splitting energies would quench the orbital angular momentum, thus suppressing the orbital contributions to the magnetism required to develop magnetic anisotropy.[12] It is logical to assume that a low coordinate number would split the d orbitals with a small separation between the electronic ground state and the excited states or within a narrow energy gap, facilitating the spin−orbital coupling to enhance the magnetic anisotropy.[5,6a,b,12,13] Indeed most of the quest for transition-metal-based SIMs is focused on low-coordinate metal species with coordination numbers of two,[5,6a,b,10] three,[6c,8a] four,[6d−g,8b−j] or five,[8k,l] which possess a large axial zero-field splitting parameters, D, and exhibit the slow magnetic relaxations. Long et al. have made significant progress in observing an record effective spin-reversal barrier of U_{eff} = 226(4) cm^{-1}, the largest yet observed for a single molecular magnet based on a transition metal, for the two-coordinate complex $[K(crypt\text{-}222)][Fe(C(SiMe_3)_3)_2]$.[5]

Eight-coordinate 3d metal complexes have been known since the early 1960s,[14a] but their magnetic properties have been rarely studied yet.[14b] We argue that the high coordination geometry may also lead to a small energy separation between the electronic spin ground state and low-lying excited state, thus facilitating the high magnetic anisotropy of Co(II), if the eight donor atoms provide a weak coordination field. Here we report that the first observed slow magnetic relaxation in the eight-coordinate Co(II) complex, $[Co^{II}(12C4)_2](I_3)_2(12C4)$ (**1**), with a distorted square antiprism geometry.

Complex **1** was prepared by the method of Meyer et al.[15] As reported by Meyer et al., the central Co^{2+} center is coordinated by eight oxygen atoms from two 12-crown-4 molecules, forming a distorted square antiprism geometry (Figure 1a).[15] The Co−O bond distances are in the range of 2.24(0)−2.29(4) Å. For the square antiprism geometry, two angle values φ and α are usually used to describe the structural features.[4d] A twist angle φ, defined as the rotation angle of one coordination square away from the eclipsed configuration to the other, is 45° for an ideal square antiprism (Figure 1b).[4d] The α, the angle between the eight metal−ligand directions and the S_8 axis passing through the metal atom, is 54.74° for the ideal square antiprism (Figure 1c).[4d] The twist angle φ of 39.07(7)° in **1** deviates significantly from 45°, exhibiting the rotation of one coordination square toward the other. The angles α are in the range of 55.69(5)-56.55(5)°, indicating the slight compressed distortion along its C_4 axis in **1**.

Received: May 23, 2014
Published: August 13, 2014

   dx.doi.org/10.1021/ja5051605 | J. Am. Chem. Soc. 2014, 136, 12213−12216

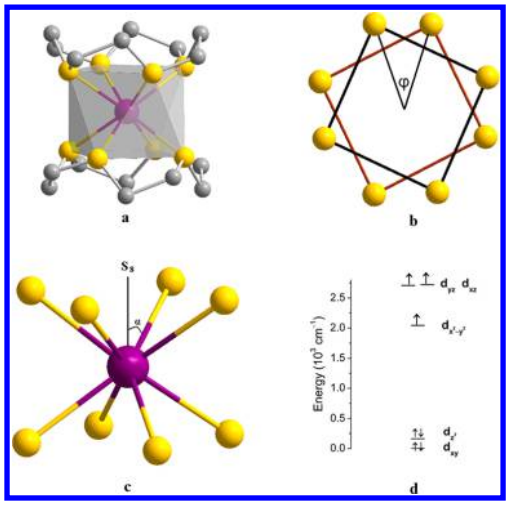

Figure 1. (a) Side view of molecular structure of the cation $[Co(12\text{-crown-}4)_2]^{2+}$ in **1**. (b) Twist angle φ defined as the rotation angle of one coordination square away from the eclipse conformation to the other. (c) The angle α defined as the eight metal−ligand bonds make with the S_8 axis passing through the metal atom Co. (d) Electronic configuration and d-orbital energy level diagram for the molecule from DFT calculation. Purple, yellow, and gray spheres represent Co, O, and C atoms, respectively. H atoms are omitted for clarity.

There is no short intermolecular exchange pathway, and this is apparent in the structure with the shortest intermolecular Co−Co distance of 10.39(0) Å (Figure S2).

To gain an insight into the electronic structure of this eight-coordinate Co(II) complex **1** with distorted square antiprism configuration, density functional theory (DFT) calculations were performed (see Supporting Information). A simple d-orbital energy diagram for this geometry is shown in Figure 1d. The partially filled orbitals (d_{xz}, d_{yz}) are nearly degenerate, resulting in a low-lying excited state which could couple with the ground state leading to a large zero-field splitting.

Variable-temperature dc susceptibility measurements were performed between 1.8 and 300 K for a powdered crystalline sample of **1** at a field of 2000 Oe (Figure S3). At 300 K, the $\chi_M T$ value is 2.79 cm^3 K mol^{-1}. It is significantly larger than the expected value of 1.875 cm^3 K mol^{-1} for an isotropic $S = 3/2$ spin center with $g = 2$, as a result of the significant orbital contribution. As the temperature is lowered, the $\chi_M T$ value remains constant down to 45 K and then rapidly decreases to 2.07 cm^3 K mol^{-1} at 1.8 K. The downturn below 45 K could probably be the magnetic anisotropy of the Co(II) ion in **1**. The experimental $\chi_M T$ data were fit using the PHI program[16] by the anisotropic Hamitonian given by the following equation (eq 1):

$$H = D(\hat{S}_z^2 - S(S+1)/3) + E(\hat{S}_x^2 - \hat{S}_y^2) + \mu_B g \hat{S} \hat{B} \quad (1)$$

Where μ_B is the Bohr magneton and D, E, S, B represent the axial and rhombic ZFS parameters, the spin operator, and magnetic field vectors, respectively. The best fit yields $D = -37.6$ cm^{-1}, $E = 0.1$ cm^{-1}, $g_{x,y} = 2.14$, and $g_z = 2.83$.

The field-dependent magnetizations were performed at applied magnetic fields of 1−7 T between 1.8 and 5.0 K (Figures S4). Using ANISOFIT 2.0[17] by diagonalizing the spin Hamiltonian (eq 1) matrix to model the M versus H/T data, the best fit afforded final parameters $g = 2.55$, $D = -38.0$ cm^{-1}, and $E = -0.75$ cm^{-1} ($f = 0.0012$) (Figure S4). Good agreement for the values of ZFS parameters obtained by simulations was observed between the $\chi_M T$ data and the M versus H/T data. To estimate the sign of D, approximate 20 fits by setting the different initial D values were attempted (Supporting Information), and the final output results are shown in Table S1. No reasonable optimization was obtained when the initial D value is positive, indicating the correct choice of the negative sign.

The EPR spectrum of complex **1** at X-band (9.4 GHz) at low temperatures (2−20 K) consists of a single peak at $g_{eff} \cong 7$. It is not instructive as to the sign and magnitude of zero-field splitting. We thus applied high-frequency and -field EPR (HFEPR) measurements on **1**.[18,19] The HFEPR frequency covered the range of 100−700 GHz, while the magnetic field varied from 0 to 25 T. The HFEPR response was extremely weak and limited to the low-frequency region (<220 GHz) where sufficient sub-THz wave power was available (Figure S5). It consisted of a single resonance at $g_{eff} \cong 7-8$ which is probably the same one visible at X-band. No other resonances were observed. A situation in which a high-spin Co(II) complex is virtually "HFEPR-silent" can occur only in a case when the $\pm 3/2$ Kramers doublet is exclusively populated at low temperatures, and the $\pm 1/2$ doublet lies much higher on the energy scale, i.e., for large negative D. A transition within the $\pm 3/2$ doublet is forbidden since $\Delta M_s = \pm 3$. While a sizable rhombic ZFS parameter E would mix the $\pm 3/2$ doublet with the $\pm 1/2$ doublet, making the intra-Kramers transition partially allowed, such as observed in the analogous $S = 3/2$ spin-state Re(IV),[11a] the absence of such an effect strongly suggests that the ZFS tensor is nearly axial. The lack of observable inter-Kramers transition(s) in the high-frequency and -field conditions between the $\pm 3/2$ and $\pm 1/2$ doublets such as detected in some other Co(II) complexes[20] puts a lower limit on $|D| > \sim 20$ cm^{-1} as obtained through simulations. This observation agrees with the lack of intra-Kramers resonances attributable to the $\pm 1/2$ doublet at low temperatures.

The zero-field splitting parameters were calculated using CASPT2 method (calculation details see Supporting Information). The calculated values are $D = -70.1$ cm^{-1}, $E = 1.05$ cm^{-1}, $g_x = 2.202$, $g_y = 2.253$, $g_z = 3.074$. The calculated large value and negative sign for D agree with the experimental data obtained from variable-temperature dc susceptibility and magnetization measurements, further demonstrating the large magnetic anisotropy of **1**. The calculated magnetic anisotropic axis coincides nearly with the C_4 axis of this molecule (Figure S6), indicating that the ligand field exhibits higher axial character in this direction than in other directions.

The large and negative D value could be attributed to the distortion of the coordination geometry of **1** in comparison to the ideal square antiprism geometry. To further probe the effect of the structural distortion in the magnetic anisotropy for complex **1**, the ZFS parameters were calculated for the assumed state with the ideal square antiprism (state **c**: $\varphi = 45$ °, $\alpha = 54.74°$) and two intermediate states (state **a**: $\varphi = 39.07°$, $\alpha = 54.74°$; state **b**: $\varphi = 45$ °, $\alpha = 55.69(5)-56.55(5)°$). Comparison of the calculated results of these three states and complex **1** suggested that the absolute value of axial ZFS parameter D decreases with the increase of angle φ and slightly increases with the increase of angle α (see the calculation details in Supporting Information). The absolute value of D for **1** is less than that for the ideal square antiprism, which could mainly be attributed to the different angle φ. These calculations suggested that the distortion with φ has greater effect in the D value of the eight-coordinate geometry.

The ac magnetic susceptibilitiy was investigated at 2 K under different external dc fields of 0−2000 Oe (Figure S8). No out-of-phase ac susceptibility (χ_M'') signal was observed under the zero

dx.doi.org/10.1021/ja5051605 | J. Am. Chem. Soc. 2014, 136, 12213−12216

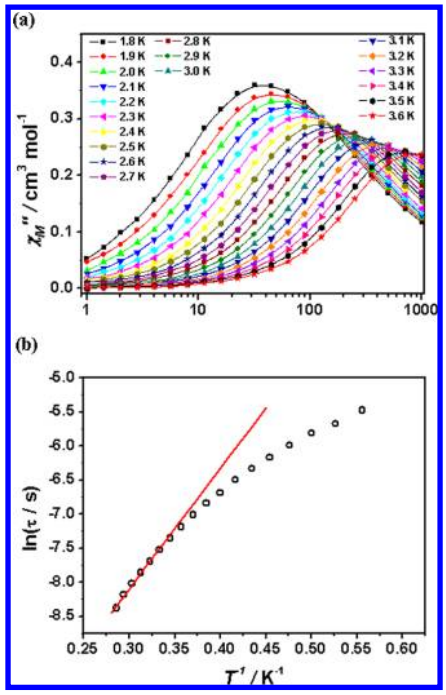

Figure 2. (a) Frequency dependence of the out-of-phase ac susceptibility from 1.8 to 3.6 K under a 500 Oe dc field for **1**. The solid lines are for eye guide. (b) Relaxation time of the magnetization $\ln(\tau)$ vs T^{-1} plot for **1**. The solid lines represent Arrhenius fits. The data were collected from the maximum of χ_M'' against frequency at different temperature.

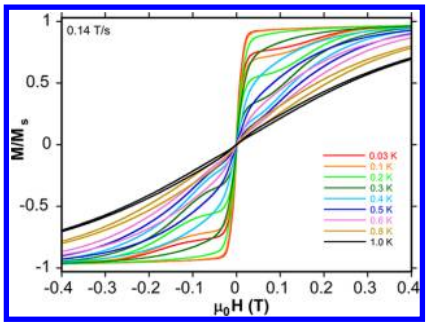

Figure 3. Field dependence of the normalized magnetization of **1** in the temperature range 0.03−1 K at field-sweep rate 0.14 T s^{-1}.

applied dc field. The absence of slow relaxation under the zero applied field should be due to quantum tunneling of the magnetization (QTM). But this phenomenon could be suppressed when a proper dc field is applied. A peak of χ_M'' signal appears at 63 Hz under a field of 200 Oe. This peak intensifies when the applied dc field is increased from 200 to 500 Oe. However, this peak moves to the high frequency with further increase of the dc field to 2000 Oe. The maximum value of the relaxation time under 500 Oe dc field was visually observed by extracting the relaxation time from the field-dependence ac susceptibility (Figure S9). Hence, additional ac measurements under 500 Oe was investigated in the temperature range of 1.8−10 K (Figures 2a and S10−12), and the temperature dependence and frequency dependence of the ac susceptibility indicated compound **1** exhibits the magnetic relaxation processes.

The peaks of out-of-phase χ_M'' from the frequency-dependent data were used to construct the Arrhenius plots, depicted in Figure 2b. A fit to the linear relationship affords an effective spin-reversal barrier U_{eff} = 17.0 cm^{-1} and a preexponential factor of τ_0 = 1.5 × 10^{-6} s. The thermally activated behavior observed at the high-temperature range are mainly attributed to an Orbach relaxation process through the excited $M_s = \pm 1/2$ levels. The region at the low temperature is likely dominated by a Raman and/or a direct phonon-based relaxation mechanisms.[6a,d,8o] In addition, the value U_{eff} of 76.0 cm^{-1} can be estimated using the barrier equation $U = |D|(S_T^2 - 1/4)$ when D is −38 cm^{-1} obtained from the magnetization measurements, which is much larger than the U_{eff} value of 17.0 cm^{-1} observed through ac susceptibility measurements. This inconsistency indicates the presence of the non-negligible QTM in these molecules. The Cole−Cole plots were generated from the ac magnetic susceptibility data and fitted using the generalized Debye model (Figure S13). The fitting parameters are summarized in Table S3. The α values are in the range of 0.06−0.32 (α indicates deviation from the pure Debye model),[21] suggesting multiple relaxation processes and the existence of the remaining QTM relaxation for complex **1**.[8o]

In order to gain further insight into the low-temperature slow magnetic relaxation behavior of complex **1**, single-crystal dc magnetization measurements were performed on a micro-SQUID magnetometer[22] between 0.03 and 5 K at scan rates of 0.004−0.280 T s^{-1} (Figures 3 and S14−S17). The field sweep rate and temperature-dependent hysteresis loops were observed, indicating complex **1** is a real SMM. Hysteresis loops were seen below 1 K, which increases with increasing sweep rate and decreasing temperature. However, the loop at 0.03 K is smaller than those at 0.1−0.5 K. Similar phenomena have been observed other Co(II)[8m,p] and Mn(III)-based[9c] SIMs, which is due to the effect of fast tunnel rate at 0.03 K. Besides, the observed closed hysteresis loop at zero dc field could be attributed to fast quantum tunneling of the magnetization, consistent with the ac magnetic susceptibility measurements. The field was aligned with the mean easy axis of magnetization using the transverse field method,[23] as depicted in Figure S17, which allows us to confirm that the anisotropy parameter D is negative.

In conclusion, we report here the first observations of the field-induced slow magnetic relaxation and hysteresis loops for a eight-coordinate mononuclear Co(II) complex **1**. *Ab initio* calculation shows the presence of a magnetic anisotropy, which was confirmed by the dc magnetic measurements. Alternative-current magnetic susceptibility measurements give the observed relaxation barrier of 17.0 cm^{-1}. We believe these results point to a new avenue to study slow magnetic relaxation in a highly coordinated environment. Future effort will focus on the effects of structural distortion and coordination number on the mononuclear Co(II) SIMs, yield a combination of a large overall barrier and a small quantum tunneling rate.

■ ASSOCIATED CONTENT

Supporting Information

Experimental, physical measurements, and computational details, additional magnetic data, and some figures including XRD pattern. This material is available free of charge via the Internet at http://pubs.acs.org.

■ AUTHOR INFORMATION

Corresponding Authors

xtchen@netra.nju.edu.cn
zhangyiquan@njnu.edu.cn
yousong@nju.edu.cn

Notes

The authors declare no competing financial interest.

■ ACKNOWLEDGMENTS

We thank the financial support from the National Basic Research Program of China (no. 2013CB922102 to X.-T.C. and Y.S.), U.S. National Science Foundation (CHE-1012173 to Z.-L.X.), and the Natural Science Foundation of Jiangsu Province of China (BK2011778 to Y.-Q.Z.). HFEPR experiments were conducted at the National High Magnetic Field Laboratory in Tallahassee, FL, which is funded by U.S. National Science Foundation (Cooperative Agreement DMR 1157490), the State of Florida, and Department of Energy. We thank Drs. J. Krzystek (National High Magnetic Field Laboratory), Joshua Telser (Roosevelt University, Chicago), and Zhenxing Wang (UCLA) for performing the HFEPR experiments.

■ REFERENCES

(1) (a) Gatteschi, D.; Sessoli, R.; Villain, J.; *Molecular Nanomagnets*; Oxford University Press: Oxford, UK, 2006;. (b) Gatteschi, D.; Sessoli, R. *Angew. Chem., Int. Ed.* **2003**, *42*, 268. (c) Wernsdorfer, W.; Sessoli, R. *Science* **1999**, *284*, 133. (d) Leuenberger, M. N.; Loss, D. *Nature* **2001**, *410*, 789. (e) Bogani, L.; Wernsdorfer, W. *Nat. Mater.* **2008**, *7*, 179.

(2) (a) Sessoli, R.; Tsai, H. L.; Schake, A. R.; Wang, S.; Vincent, J. B.; Folting, K.; Gatteschi, D.; Christou, G.; Hendrickson, D. N. *J. Am. Chem. Soc.* **1993**, *115*, 1804. (b) Bagai, R.; Christou, G. *Chem. Soc. Rev.* **2009**, *38*, 1011. (c) Sessoli, R.; Gatteschi, D.; Caneschi, A.; Novak, M. A. *Nature* **1993**, *365*, 141. (d) Gatteschi, D.; Sessoli, R.; Cornia, A. *Chem. Commun.* **2000**, *9*, 725. (e) Murrie, M. *Chem. Soc. Rev.* **2010**, *39*, 1986.

(3) Ishikawa, N.; Sugita, M.; Ishikawa, T.; Koshihara, S.; Kaizu, Y. *J. Am. Chem. Soc.* **2003**, *125*, 8694.

(4) (a) Guo, Y.-N.; Xu, G.-F.; Guo, Y.; Tang, J. K. *Dalton Trans.* **2011**, *40*, 9953. (b) Zhang, P.; Guo, Y.-N.; Tang, J. K. *Coord. Chem. Rev.* **2013**, *257*, 1728. (c) Woodruff, D. N.; Winpenny, R. E. P.; Layfield, R. A. *Chem. Rev.* **2013**, *113*, 5110. (d) Sorace, L.; Benelli, C.; Gatteschi, D. *Chem. Soc. Rev.* **2011**, *40*, 3092. (e) Zhang, P.; Zhang, L.; Wang, C.; Xue, S.-F.; Lin, S.-Y.; Tang, J.-K. *J. Am. Chem. Soc.* **2014**, *136*, 4484. (f) Guo, Y.-N.; Xu, G.-F.; Gamez, P.; Zhao, L.; Lin, S.-Y.; Deng, R. P.; Tang, J. K.; Zhang, H.-J. *J. Am. Chem. Soc.* **2010**, *132*, 8538. (g) Guo, Y.-N.; Xu, G.-F.; Wernsdorfer, W.; Ungur, L.; Guo, Y.; Tang, J. K.; Zhang, H.-J.; Chibotaru, L. F.; Powell, A. K. *J. Am. Chem. Soc.* **2011**, *133*, 11948.

(5) Zadrozny, J. M.; Xiao, D. J.; Atanasov, M.; Long, G. J.; Grandjean, F.; Neese, F.; Long, J. R. *Nat. Chem.* **2013**, *5*, 577.

(6) (a) Zadrozny, J. M.; Atanasov, M.; Bryan, A. M.; Lin, C.-Y.; Rekken, B. D.; Power, P. P.; Neese, F.; Long, J. R. *Chem. Sci.* **2013**, *4*, 125. (b) Atanasov, M.; Zadrozny, J. M.; Long, J. R.; Neese, F. *Chem. Sci.* **2013**, *4*, 139. (c) Lin, P.-H.; Smythe, N. C.; Gorelsky, S. I.; Maguire, S.; Henson, N. J.; Korobkov, I.; Scott, B. L.; Gordon, J. C.; Baker, R. T.; Murugesu, M. *J. Am. Chem. Soc.* **2011**, *133*, 15806. (d) Freedman, D. E.; Harman, W. H.; Harris, T. D.; Long, G. J.; Chang, C. J.; Long, J. R. *J. Am. Chem. Soc.* **2010**, *132*, 1224. (e) Harman, W. H.; Harris, T. D.; Freedman, D. E.; Fong, H.; Chang, A.; Rinehart, J. D.; Ozarowski, A.; Sougrati, M. T.; Grandjean, F.; Long, G. J.; Long, J. R.; Chang, C. J. *J. Am. Chem. Soc.* **2010**, *132*, 18115. (f) Weismann, D.; Sun, Y.; Lan, Y.; Wolmershäuser, G.; Powell, A. K.; Sitzmann, H. *Chem.—Eur. J.* **2011**, *17*, 4700. (g) Mathonière, C.; Lin, H.-J.; Siretanu, D.; Clérac, R.; Smith, J. M. *J. Am. Chem. Soc.* **2013**, *135*, 19083. (h) Feng, X.; Mathonière, C.; Jeon, I.-R.; Rouzières, M.; Ozarowski, A.; Aubrey, M. L.; Gonzalez, M. I.; Clérac, R.; Long, J. R. *J. Am. Chem. Soc.* **2013**, *135*, 15880.

(7) Mossin, S.; Tran, B. L.; Adhikari, D.; Pink, M.; Heinemann, F. W.; Sutter, J.; Szilagyi, R. K.; Meyer, K.; Mindiola, D. J. *J. Am. Chem. Soc.* **2012**, *134*, 13651.

(8) (a) Eichhöfer, A.; Lan, Y.; Mereacre, V.; Bodenstein, T.; Weigend, F. *Inorg. Chem.* **2014**, *53*, 1962. (b) Zadrozny, J. M.; Long, J. R. *J. Am. Chem. Soc.* **2011**, *133*, 20732. (c) Zadrozny, J. M.; Liu, J. J.; Piro, N. A.; Chang, C. J.; Hill, S.; Long, J. R. *Chem. Commun.* **2012**, *48*, 3897. (d) Buchholz, A.; Eseola, A. O.; Plass, W. *C. R. Chim.* **2012**, *15*, 929. (e) Gomez-Coca, S.; Cremades, E.; Aliaga-Alcalde, N.; Ruiz, E. *J. Am. Chem. Soc.* **2013**, *135*, 7010. (f) Yang, F.; Zhou, Q.; Zhang, Y. Q.; Zeng, G.; Li, G. H.; Shi, Z.; Wang, B. W.; Feng, S. H. *Chem. Commun.* **2013**, *49*, 5289. (g) Cao, D.-K.; Feng, J.-Q.; Ren, M.; Gu, Y.-W.; Song, Y.; Ward, M. D. *Chem. Commun.* **2013**, *49*, 8863. (h) Zadrozny, J. M.; Telser, J.; Long, J. R. *Polyhedron* **2013**, *64*, 209. (i) Huang, W.; Liu, T.; Wu, D. Y.; Cheng, J. J.; Ouyangc, Z. W.; Duan, C. Y. *Dalton Trans.* **2013**, *42*, 15326. (j) Boča, R.; Miklovič, J.; Titiš, J. *Inorg. Chem.* **2014**, *53*, 2367. (k) Jurca, T.; Farghal, A.; Lin, P.-H.; Korobkov, I.; Murugesu, M.; Richeson, D. S. *J. Am. Chem. Soc.* **2011**, *133*, 15814. (l) Habib, F.; Luca, O. R.; Vieru, V.; Shiddiq, M.; Korobkov, I.; Gorelsky, S. I.; Takase, M. K.; Chibotaru, L. F.; Hill, S.; Crabtree, R. H.; Murugesu, M. *Angew. Chem., Int. Ed.* **2013**, *52*, 11290. (m) Vallejo, J.; Castro, I.; Ruiz-García, R.; Cano, J.; Julve, M.; Lloret, F.; De Munno, G.; Wernsdorfer, W.; Pardo, E. *J. Am. Chem. Soc.* **2012**, *134*, 15704. (n) Zhu, Y.-Y.; Cui, C.; Zhang, Y.-Q.; Jia, J.-H.; Guo, X.; Gao, C.; Qian, K.; Jiang, S.-D.; Wang, B.-W.; Wang, Z.-M.; Gao, S. *Chem. Sci.* **2013**, *4*, 1802. (o) Chandrasekhar, V.; Dey, A.; Mota, A. J.; Colacio, E. *Inorg. Chem.* **2013**, *52*, 4554. (p) Colacio, E.; Ruiz, J.; Ruiz, E.; Cremades, E.; Krzystek, J.; Carretta, S.; Cano, J.; Guidi, T.; Wernsdorfer, W.; Brechin, E. K. *Angew. Chem., Int. Ed.* **2013**, *52*, 9130. (q) Herchel, R.; Váhovská, L.; Potočňák, I.; Trávníček, Z. *Inorg. Chem.* **2014**, *53*, 5896. (r) Wu, D. Y.; Zhang, X. X.; Huang, P.; Huang, W.; Ruan, M. Y.; Ouyang, Z. W. *Inorg. Chem.* **2013**, *52*, 10976.

(9) (a) Ishikawa, R.; Miyamoto, R.; Nojiri, H.; Breedlove, B. K.; Yamashita, M. *Inorg. Chem.* **2013**, *52*, 8300. (b) Grigoropoulos, A.; Pissas, M.; Papatolis, P.; Psycharis, V.; Kyritsis, P.; Sanakis, Y. *Inorg. Chem.* **2013**, *52*, 12869. (c) Vallejo, J.; Pascual-Alvarez, A.; Cano, J.; Castro, I.; Julve, M.; Lloret, F.; Krzystek, J.; De Munno, G.; Armentano, D.; Wernsdorfer, W.; Ruiz-Garcia, R.; Pardo, E. *Angew. Chem., Int. Ed.* **2013**, *52*, 14075.

(10) Poulten, R. C.; Page, M. J.; Algarra, A. G.; Le Roy, J. J.; López, I.; Carter, E.; Llobet, A.; Macgregor, S. A.; Mahon, M. F.; Murphy, D. M.; Murugesu, M.; Whittlesey, M. K. *J. Am. Chem. Soc.* **2013**, *135*, 13640.

(11) (a) Martnez-Lillo, J.; Mastropietro, T. F.; Lhotel, E.; Paulsen, C.; Cano, J.; De Munno, G.; Faus, J.; Lloret, F.; Julve, M.; Nellutla, S.; Krzystek, J. *J. Am. Chem. Soc.* **2013**, *135*, 13737. (b) Pedersen, K. S.; Sigrist, M.; Søensen, M. A.; Barra, A.-L.; Weyhermüller, T.; Piligkos, S.; Thuesen, C. A.; Vinum, M. G.; Mutka, H.; Weihe, H.; Clérac, R.; Bendix, J. *Angew. Chem. Int., Ed.* **2014**, *53*, 1351.

(12) Dey, M.; Gogoi, N. *Angew. Chem., Int. Ed.* **2013**, *52*, 12780.

(13) Power, P. P. *Chem. Rev.* **2012**, *112*, 3482.

(14) (a) Lippard, S. J. Eight-Coordination Chemistry. In *Prog. Inorg. Chem.*; Cotton, F. A., Eds.; John Wiley & Sons: New York, 1967; Vol. *8*, pp 109−156. (b) Garner, C. D.; Mabbs, F. E. *J. Chem. Soc., Dalton Trans.* **1976**, 525.

(15) Fiolka, C.; Pantenburg, I.; Meyer, G. *Cryst. Growth Des.* **2011**, *11*, 5159.

(16) Chilton, N. F.; Anderson, R. P.; Turner, L. D.; Soncini, A.; Murray, K. S. *J. Comput. Chem.* **2013**, *34*, 1164.

(17) Shores, M. P.; Sokol, J. J.; Long, J. R. *J. Am. Chem. Soc.* **2002**, *124*, 2279.

(18) Zvyagin, S. A.; Krzystek, J.; van Loosdrecht, P. H. M.; Dhalenne, G.; Revcolevschi, A. *Phys. B (Amsterdam, Neth.)* **2004**, *346−347*, 1.

(19) Hassan, A. K.; Pardi, L. A.; Krzystek, J.; Sienkiewicz, A.; Goy, P.; Rohrer, M.; Brunel, L. C. *J. Magn. Reson.* **2000**, *142*, 300.

(20) Krzystek, J.; Swenson, D. C.; Zvyagin, S. A.; Smirnov, D.; Ozarowski, A.; Telser, J. *J. Am. Chem. Soc.* **2010**, *132*, 5241.

(21) (a) Cole, K. S.; Cole, R. H. *J. Chem. Phys.* **1941**, *9*, 341. (b) Aubin, S. M.; Sun, Z.; Pardi, L.; Krzystek, J.; Folting, K.; Brunel, L. C.; Rheingold, A. L.; Christou, G.; Hendrickson, D. N. *Inorg. Chem.* **1999**, *38*, 5329.

(22) Wernsdorfer, W. *Adv. Phys. Chem.* **2001**, *118*, 99.

(23) Wernsdorfer, W.; Chakov, N. E.; Christou, G. *Phys. Rev. B* **2004**, *70*, 132413.